Geophysical Research Letters

RESEARCH LETTER
10.1029/2021GL095357

Special Section:
Understanding carbon-climate feedbacks

Evaluation of Radiocarbon ^{14}C Yield Under Conditions of Thunderstorms

V. I. Lyashuk[1,2]

[1]Institute for Nuclear Research of the Russian Academy of Sciences, Moscow, Russia, [2]National Research Center "Kurchatov Institute", Moscow, Russia

Key Points:

- The gross model for evaluation of the radiocarbon ^{14}C creation during thunderstorms
- Probability of ^{14}C generation in the atmosphere depending on the neutron energy
- Radiocarbon creation under thunderstorms at different altitudes. Comparison with ^{14}C yield from the cosmic irradiation

Supporting Information:

Supporting Information may be found in the online version of this article.

Correspondence to:

V. I. Lyashuk,
lyashuk@itep.ru

Citation:

Lyashuk, V. I. (2021). Evaluation of radiocarbon ^{14}C yield under conditions of thunderstorms. *Geophysical Research Letters*, *48*, e2021GL095357. https://doi.org/10.1029/2021GL095357

Received 26 JUL 2021
Accepted 19 OCT 2021

Author Contributions:

Conceptualization: V. I. Lyashuk
Data curation: V. I. Lyashuk
Formal analysis: V. I. Lyashuk
Investigation: V. I. Lyashuk
Methodology: V. I. Lyashuk
Project Administration: V. I. Lyashuk
Resources: V. I. Lyashuk
Software: V. I. Lyashuk
Supervision: V. I. Lyashuk
Validation: V. I. Lyashuk
Visualization: V. I. Lyashuk
Writing – original draft: V. I. Lyashuk
Writing – review & editing: V. I. Lyashuk

Abstract

The knowledge of radioactive ^{14}C yield under atmospheric thunderstorm flash conditions (the additional channel of ^{14}C production relative to the main cosmogenic one) is important for radiocarbon analysis. A gross model for evaluation of the thunderstorm ^{14}C yield simulated for the altitudes up to 15 km is proposed. It was observed that yield from the thunderstorm mechanisms of ^{14}C creation cannot compete with cosmogenic production which is six orders of value larger. The obtained result allows us to eliminate the problematic issue on thunderstorm radiocarbon generation in the atmosphere as the additional significant source.

Plain Language Summary

The creation of isotopes takes place not only in stellar conditions but also in the Earth's atmosphere under cosmic irradiation. Radioactive carbon ^{14}C produced in the atmosphere is an exclusively important tool for historical dating (in archeology, glaciology, biology, paleontology, geology, Sun activity and climate in the past) for the time scale up to ~(50–60) thousands of years. But radiocarbon creation is also possible from thunderstorm discharges. In case of significant yield, it will cause the correction of dating results. To solve this problem, the model that takes into account the rate of ^{14}C production depending on the part of energetic electrons in the thunderstorm flash discharges for different altitudes is proposed. The probability of ^{14}C creation depending on the energy of neutrons generated under thunderstorms was calculated. The results revealed that yield of thunderstorm mechanism is very small when compared to the main one originated from the cosmic irradiation. It allows us to eliminate the problematic question on the correction arising from this additional source of ^{14}C isotope. The reliability of the obtained results is confirmed by simulation of the Japan experiment on neutron registration at the strong thunderstorm in January 5 2012.

1. Introduction

The main mechanism of radiocarbon ^{14}C creation in the Earth's atmosphere is ensured by cosmogenic irradiation with a yield of 472 g-mole/year (Roth & Joos, 2013) in the reaction $^{14}N(n,p)^{14}C$. The generated isotope of ^{14}C is assimilated in the biomass and decays within it ($T_{1/2}$ = 5700 years) that allows us to date the age of investigated organic materials. Discovery of short-term secular fluctuations of radiocarbon in tree rings (Suess, 1965) and its correlation with sun spot number had raised questions that should be eliminated to explain the nature of the phenomenon. In addition to the solar mechanism of fluctuations, the hypothesis of short-term ^{14}C variation under thunderstorm generated neutrons in fusion reaction $^2H + {}^2H \rightarrow {}^3He + n$ (due to acceleration of deuterium ions at lightning discharges) with a yield of ≃2.5 MeV neutrons (Libby & Lukens, 1973) was proposed. But the deuterium concentration in the atmospheric H_2O vapor is small (1 ^2H nucleus per ~10^4 ^1H nuclei) (Rozansky & Sonntag, 1982; Gerst & Quay, 2000), and the maximal electric field strength inside the thunderclouds (~1×10^6 V/m) (Winn et al., 1974; Gunn, 1948) is too small for evident neutron generation, which results in negligible neutron creation (Babich, 2006); in conclusion, the fusion cannot be responsible for short-term radiocarbon fluctuation. Nevertheless, indications of the low-rate fusion are obtained; so, the authors of the experiment at the High Altitude Research Laboratory (India) registered that 2.45 MeV neutrons correlated with lightning strokes (Ishtiaq et al., 2016).

The first evidence of thunderstorm neutron enrichment was obtained in high-altitude Himalayas experiment (Shah et al., 1985). The enrichment of neutron fluxes, γ- and X-rays in correlation with thunderstorms were also registered in the following experiments (as: Chilingarian et al., 2010; Kuzhevskii, 2004; Shyam & Kaushik, 1999; Starodubtsev et al., 2012).

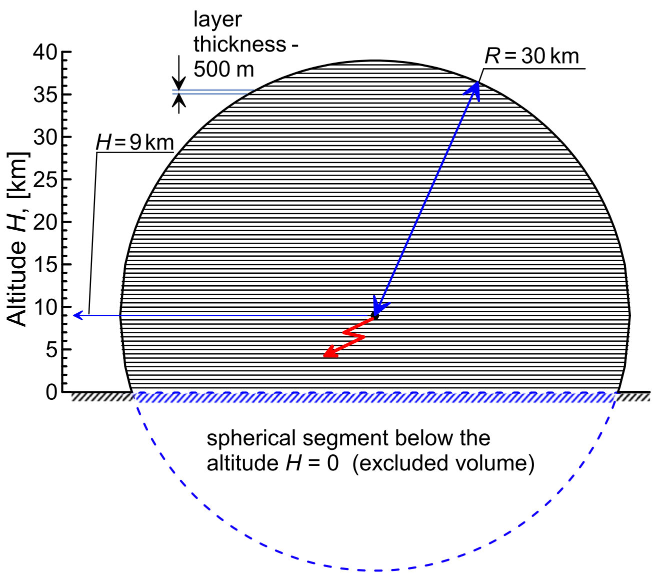

Figure 1. Geometry of the spherical-layers model for simulation of the particles transport and radiocarbon ^{14}C creation in the air under conditions of thunderstorms lightning [example for lightning (indicated as red arrow) originated at altitude $H = 9$ km on the sea level]. The spherical segment below the sea level ($H = 0$) is excluded from the ^{14}C accumulation process.

The breakthrough in understanding of lightning and correlated irradiation happened, thanks to the idea of relativistic electron avalanche created under atmospheric electric fields conditions (Gurevich et al., 1992). The electron avalanche develops under strong cloud electric conditions (Dwyer & Babich, 2011; Gurevich et al., 2006) and can be initiated by high-energy cosmic particles (Chilingarian et al., 2014).

The electron energy spreads up to tens of MeV ensuring the multiplication of the avalanche. Relativistic electrons ($E > 1$ MeV) move in the forward part of the lightning discharge generating low-energy electrons in interactions (via ionization), drawing them into the avalanche accelerated in the thunderstorm electric field. In contrast, the electrons with energy below the threshold ($\simeq$100 eV) fall out from the avalanche, forming the dynamical equilibrium between involved and lost electrons. An investigation of electron acceleration in electric fields was initiated by Wilson almost a century ago (Wilson, 1925).

The electrons in the discharge avalanche slow down and escape photons (bremsstrahlung) which in turn produce photo-neutrons in $^{14}N(\gamma,n)$-reaction. Radiocarbon synthesis $^{14}N(n,p)^{14}C$ under atmospheric thunderstorms conditions goes at the end of process chain (Babich & Roussel-Duprè, 2007; Babich, 2017a, 2017b). In 2017, the phenomenon of neutron production in (γ,n)-process and creation of isotopes (^{13}C, ^{13}N, ^{15}N, ^{15}O) at thunderstorms were confirmed experimentally that inevitable means the radiocarbon ^{14}C creation too (Enoto et al., 2017).

2. Method

2.1. The Gross Model for Particle Transport Simulation in the Atmosphere

Simulation of the particle transport and isotopes production starts with escape of electrons of energetic spectrum applied as $f \propto \exp(-\varepsilon/7.3$ [MeV]; Dwyer & Babich, 2011), where ε is the energy of the runaway electrons (i.e., electrons accelerated in electric fields of thunderclouds). The spectrum spreads up to $\simeq$60 MeV. In the avalanche, the number of low energy electrons N_{le} strongly exceeds the relativistic ones N_{re}. At altitude H, the minimal relation $R1 = N_{le}/N_{re}$ is equal to $\simeq(1.3 \times 10^4) \times n$, where $n = \rho(H)/\rho(H = 0)$, $\rho(H)$ is air density relative to the sea level $H = 0$ (Dwyer & Babich, 2011). So, the total charge of lightning is ensured almost entirely by low energy electrons and the portion of which decreases in the avalanche for higher altitudes.

Taking into account the dependence of relation N_{le}/N_{re} from the air density, the simulation was realized for the altitudes from the sea level up to the $H = 15$ km (the upper charge layer of thunderclouds at typical elevation $H = (10 \div 14)$ km; Rakov & Uman, 2005). In this model, we use the spherical geometry with centers (the point source of energetic electrons of isotropic f-spectrum) on the indicated altitudes (Figure 1).

The spheres are divided into horizontal plane layers (of 500 m thickness) with air density ρ corresponding to the layers heights. In order to prevent the escape of a valuable part of neutrons (which is born in the sphere in the threshold 14N(γ,Xn)-process, where Xn—emission of X = 1, 2, or more neutrons; $E_{threshold} = 10.6$ MeV (Shibata et al., 2002) from the geometry, the sphere radii R are increased up to 30 km. It prevented the neutron loss that is especially critical for the high-energy spectrum part. As a result, the percent of the escaping neutrons reduced below 1% relative to the total number of created photoneutrons. In addition to neutron generation in γ-interaction with ^{14}N, the yields from $^{16}O(\gamma,Xn)^{15}O$ ($E_{threshold} = 15.7$ MeV; Iwamoto et al., 2016) and $^{40}Ar(\gamma,Xn)^{39}Ar$ ($E_{threshold} = 10.0$ MeV; ENDF-7u, 2008) reactions are accounted. Therefore, it is observed that ^{14}N, ^{16}O and ^{40}Ar isotopes are responsible for yields of 75.3%, 15.7% and 9% of the all created photo-neutrons correspondingly.

The example of calculated neutron spectrum at $H = 10$ km and cross section of the $^{14}N(\gamma,Xn)$-reaction are given in Figure S1 where the expected coincidence of the maximum in neutron spectrum with maximal cross section at $E_\gamma = 23$ MeV is clearly visible. In this scenario, the total number of created neutrons amounts

10.1029/2021GL095357

1.8×10^{10} per 1 coulomb of the lightning discharge. For investigating of radiocarbon production $^{14}N(n,p)^{14}C$ at thunderstorm under photoneutron fluences, it was taken into account all of the above-mentioned processes and simulated in detail the electron, photon, and neutron transport in the model based on MCNPX code (editor: Pelowitz, 2008). As photoneutrons production in the atmosphere goes in the threshold reactions, it is reasonable to ignore the bremsstrahlung irradiation of energy below the minimal threshold (10 MeV).

2.2. Probability of Radiocarbon Production in 14N(n,p)14C

At neutron transport, the reaction $^{14}N(n,p)^{14}C$ of radiocarbon generation competes with processes of neutron captures on the air isotopes; their composition is practically stable at change of the altitude H (COESA Working Group, 1976). Then, for created neutrons, the energy dependence of probability to produce the radiocarbon is given by the relation of $^{14}N(n,p)^{14}C$ macro cross section to the total macro cross section of neutron disappearance (n,disap) in the air:

$$P(E) = \frac{\sigma^{macro}_{14N(n,p)14C}(E)}{\sigma^{macro}_{(n,\,disap)}(E)}, \tag{1}$$

$$\sigma^{macro}_{(n,\,disap)}(E) = \sum_i \left[\begin{pmatrix} \sigma^{micro,\,i}_{(n,\gamma)}(E) + \sigma^{micro,\,i}_{(n,p)}(E) + \sigma^{micro,\,i}_{(n,d)}(E) + \sigma^{micro,\,i}_{(n,t)}(E) + \sigma^{micro,\,i}_{(n,3He)}(E) + \\ \sigma^{micro,\,i}_{(n,a)}(E) + \sigma^{micro,\,i}_{(n,2a)}(E) + \sigma^{micro,\,i}_{(n,3a)}(E) + \sigma^{micro,\,i}_{(n,2p)}(E) + \sigma^{micro,\,i}_{(n,p+a)}(E) + \\ \sigma^{micro,\,i}_{(n,t+2a)}(E) + \sigma^{micro,\,i}_{(n,d+2a)}(E) + \sigma^{micro,\,i}_{(n,p+d)}(E) + \sigma^{micro,\,i}_{(n,p+t)}(E) + \sigma^{micro,\,i}_{(n,d+a)}(E) \end{pmatrix} \times n_i \right], \tag{2}$$

where $\sigma^{macro}_{14N(n,p)C14}(E) = \sigma^{micro}_{14N(n,p)C14}(E) \times n_{14N}$, and $\sigma^{micro}_{14N(n,p)14C}(E)$ – micro cross sections of $^{14}N(n,p)^{14}C$ process, and n_{14N} – nuclear concentration of ^{14}N isotope. Macro cross section of neutron disappearance in the air is calculated as the sum of indicated micro cross sections (of the reactions leading to neutron disappearance) for the ith isotope multiplied by its nuclear concentration n_i. Owing to the stable air composition for calculation of probability $P(E)$, the isotope concentration can be taken at the sea level $H = 0$.

The behavior of micro cross sections (for all channels of neutron disappearance and (n,disap) – sum of these channels) from the energy for the main air isotopes ^{14}N, ^{16}O and also ^{40}Ar (with 78.14%, 21.03%, and 0.47% yield to the total nuclear concentration correspondingly) is presented in Figures 2a–2c for the energy interval from 60 MeV down to 0.01 eV (i.e., covering all possible energies of neutrons production and then slow down to thermalization and absorption). The probability of radiocarbon production strongly depends on the neutron energy and competitive reactions. The nuclear data libraries used for plots of Figure 2 are indicated in Table S1.

At the energy $E_n \gtrsim 1$ MeV, the threshold reactions (with yield of p, a, d, t-particles) go with significant cross sections [see Figure 2a–2c]. In the energy intervals ~(0.3 ÷ 7) MeV for ^{14}N, ~(0.4 ÷ 7) MeV for ^{16}O and ~(0.01 ÷ 1) MeV for ^{40}Ar, the cross sections are described by strong resonances [in reactions: (n,p), (n,a), and (n,γ) for ^{14}N; (n,γ) and (n,a) for ^{16}O; (n,γ) for ^{40}Ar], which can be carefully processed by resonance integrals in the multigroup method used for neutron transport. Below the resonance regions (at energies: $E_n \lesssim 1 \times 10^{-1}$ MeV for ^{14}N, $E_n \lesssim 1 \times 10^{-4}$ MeV for ^{16}O, and $E_n \lesssim 1 \times 10^{-3}$ MeV for ^{40}Ar), the cross sections of neutron disappearance reactions [(n,p) and (n,γ) for ^{14}N; (n,γ) for ^{16}O and ^{40}Ar] follow to 1/V low (where V– neutron velocity), but the yield of ^{14}N(n,p)-process strongly dominates in total neutron disappearance in air.

With good precision, it is possible to consider the probability to produce the radiocarbon as

$$P(E) = \frac{\sigma^{macro}_{14N(n,p)14C}(E)}{\left[\sigma^{macro}_{14N(n,disap)}(E) + \sigma^{macro}_{16O(n,disap)}(E) + \sigma^{macro}_{40Ar(n,disap)}(E)\right]}. \tag{3}$$

The macro cross section of ^{14}N(n,p) reaction and macro cross sections of neutron disappearance in reactions with ^{14}N, ^{16}O, and ^{40}Ar (as the main air isotopes) are presented in Figures 3a and 3b for the altitude $H = 0$. The summary macro cross section of these main isotopes is indicated in Figure 3c as the $\sigma^{macro}_{(n,disap)}(\mathrm{Air})$. It is observed that at energy $E_n \lesssim 1$ MeV, the main yield to the (n,disap)-macro cross section of air is ensured

10.1029/2021GL095357

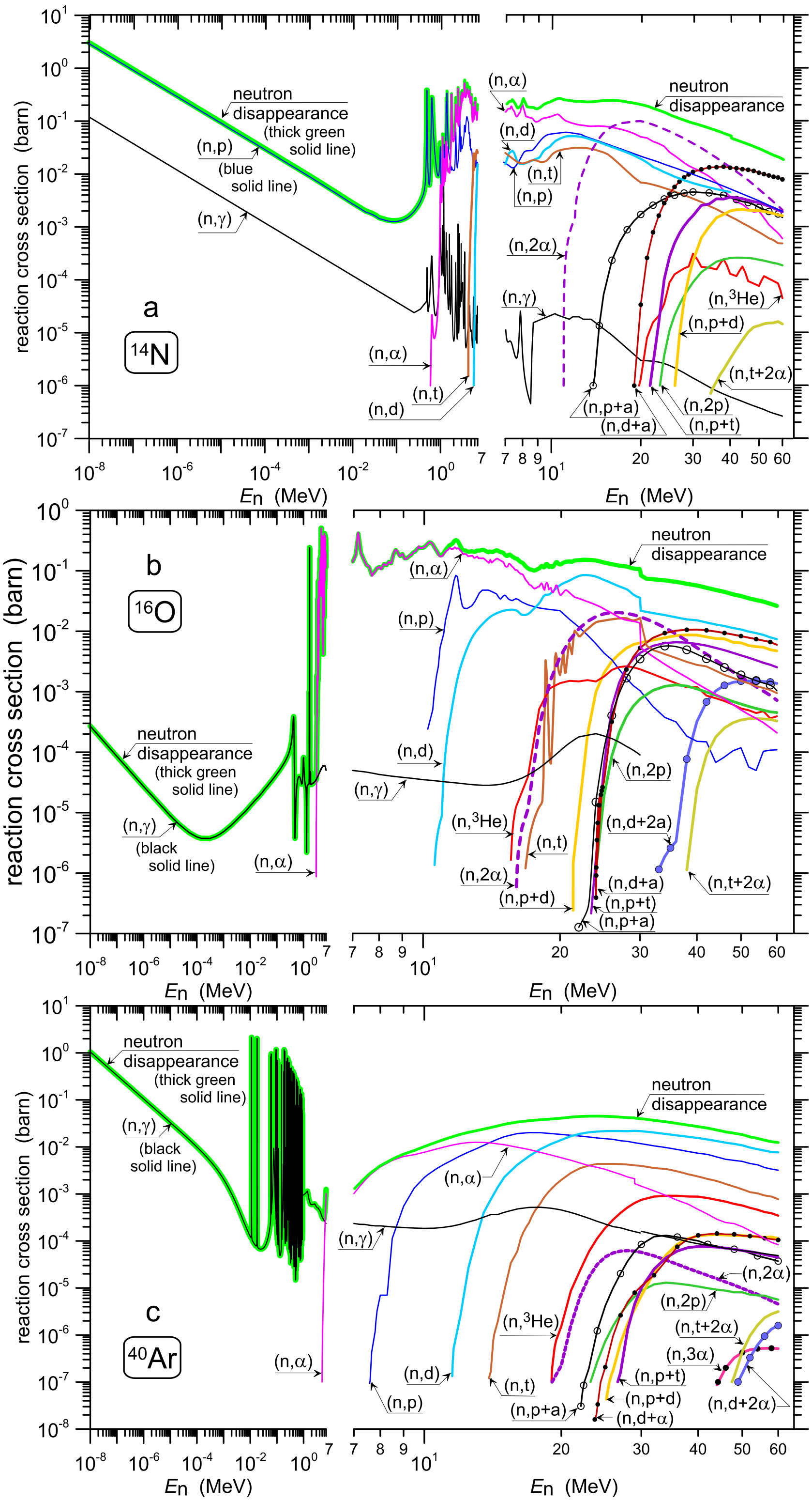

Figure 2. (a)–(c). Dependence of the (n, disappearance)-micro cross sections from the energy for the nitrogen ^{14}N, oxygen ^{16}O, and argon ^{40}Ar. The sum of (n, disap) micro cross section is shown by thick green line. For visualization, the dependencies are given in two energy scales with break at $E_n = 7$ MeV.

10.1029/2021GL095357

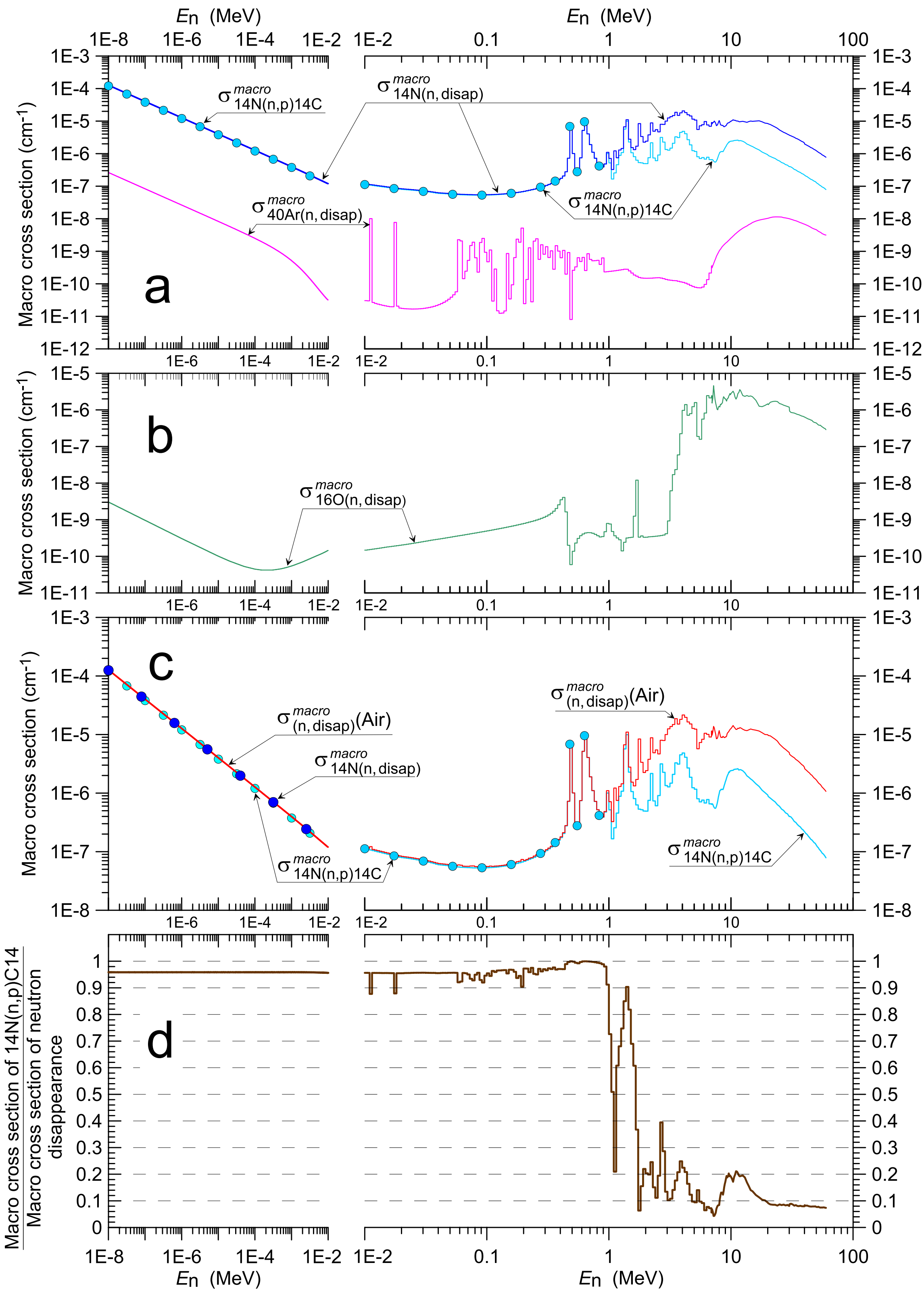

Figure 3.

10.1029/2021GL095357

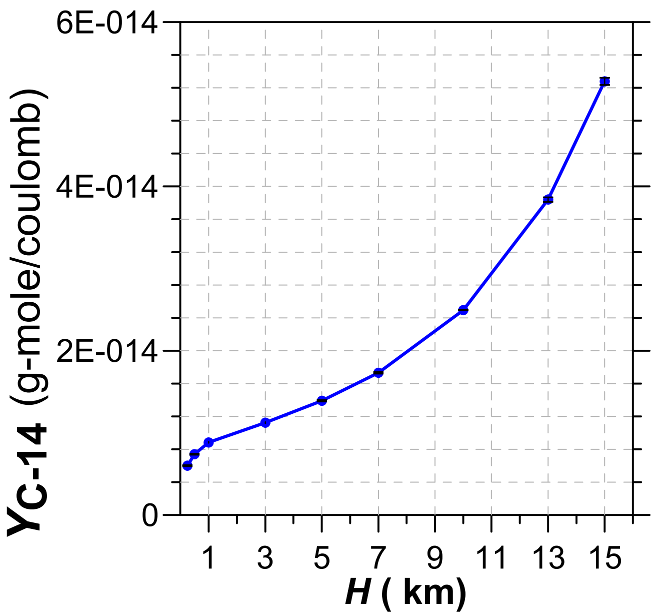

Figure 4. Yields of radiocarbon ^{14}C depending on the altitude H (km) under thunderstorm conditions. The yields (in gram-molecules) correspond to one coulomb of lightning discharge. The yields correspond to the electron avalanche model of (Dwyer & Babich, 2011).

by $^{14}N(n,p)$-reaction [see Figure 3c]. But at $E_n \gtrsim 1$ MeV (the energy region of resonances and threshold reactions), the $\sigma^{macro}_{14N(n,p)14C}$ is lower than $\sigma^{macro}_{disap}(\mathrm{Air})$ from several times to order of value. The precise probability $P(E)$ to product the radiocarbon ^{14}C is given in the Figure 3d. At energy $E_n \lesssim 1$ MeV, the P-values lay within ~(0.96 ÷ 1)-interval and strongly decrease down to $P \sim 0.1$ at larger energies.

3. Results

3.1. Evaluation of the Radiocarbon ^{14}C Yield

For calculation of the radiocarbon ^{14}C yield, the volumes of the spherical segments below $H = 0$ (dashed line in Figure 1) are excluded from the considered volumes. Such a spherical-plane-layer formalism allowed us to specify the fraction $N_{re}/(N_{le} + N_{re})$ of relativistic electrons N_{re} (responsible for ^{14}C production for the current altitude H) in the total $(N_{le} + N_{re})$-flux and to obtain the ^{14}C yields depending on the altitudes (see Figure 4).

The $^{14}N(n,p)$ ^{14}C radiocarbon yields are ensured by part P_{escape} of neutrons which escape the disappearance in the other (n,disap)-reactions [listed in Equation 2, Figures 2a–2c] at slowing down and diffusion. So, for the altitude $H = 10$ km, it was found that $P_{\mathrm{escape}} = 0.83$.

The drop of the low energy population N_{le} in the avalanche at the increase of the altitude ensures rise of ^{14}C yield (for equal lightning charges values). All presented results of isotope generation (in gramme-molecules) are normalized per 1 coulomb. If the discharge occurs between thunderclouds in the horizontal layer (in the model geometry; Figure 1) at the same altitude H_{fix}, then the normalized yield corresponds to the function $Y(H_{\mathrm{fix}})$ as shown in Figure 4. In this model, the discharge within the horizontal layer can be presented as "movement" of the geometry-model-sphere in the same direction (as discharge movement) as that for the indicated task (altitude dependent ^{14}C yield evaluation) is equivalent to the fix position of this sphere at the altitude of the discharge. In the common case, the discharge propagates between some altitudes H_1 and H_2. Then, the ^{14}C yield is calculated as the integral along the discharge path S: $Y = \int_S p\left(x, y, H\right) ds$, where $p\left(x, y, H\right)$ is the density of radiocarbon generation at the discharge in the $\left(x, y, H\right)$-coordinates, which depends on time t as the parameter (i.e., $p\left(x, y, H\right) \equiv p\left[x\left(t\right), y\left(t\right), H\left(t\right)\right]$). If it is assumed that $[N_{re}/(N_{le} + N_{re})]$ depends only on the altitude H (i.e., this relation is stable in time, and the condition for discharges does not change in x-y–plane), then $p\left[x\left(t\right), y\left(t\right), H\left(t\right)\right] = p\left[H\left(t\right)\right]$. As a result, the ^{14}C yield is calculated as $Y = \int_{\Delta t} p\left[H\left(t\right)\right] dt$ during the discharge time Δt. For the discharge propagated between altitudes H_1 and H_2 (where $H_2 > H_1$), the radiocarbon yield Y will be the following:

$$Y\left(H_1\right) = \int_{\Delta t} p\left[H_1\right] dt < Y < Y\left(H_2\right) = \int_{\Delta t} p\left[H_2\right] dt \quad . \tag{4}$$

Let us evaluate the ^{14}C production per year under the lightning conditions (using the data of Figure 4; knowing that the number of lightning on the Earth per 1 year is 1.4×10^9 (Christian et al., 2003); considering that the average lightning charge is ~20 coulombs (Rakov & Uman, 2005), allowing the mean altitude

Figure 3. (a) Dependence of (n, disappearance)-macro cross sections of the air isotopes (^{14}N and ^{40}Ar) from the energy (dark blue and violet solid lines correspondingly). Dependence of macro cross section for radiocarbon creation $^{14}N(n,p)^{14}C$ from the energy (light blue circles ● at $E_n \lesssim 0.85$ MeV and light blue solid line at $E_n \gtrsim 0.85$ MeV). (b) Dependence of (n, disap)-macro cross section of the air isotope ^{16}O from the energy (solid lines). (c) Dependence of the summary (n, disap)-macro cross section of the air isotopes (^{14}N, ^{16}O and ^{40}Ar) from the energy is denoted as $\sigma^{macro}_{disap}(\mathrm{Air})$ (red solid lines). Dependence of macro cross section for $^{14}N(n,p)^{14}C$-reaction from the energy (light blue circles ● at $E_n \lesssim 0.85$ MeV and light blue solid line at $E_n \gtrsim 0.85$ MeV). Dependence of $\sigma^{macro}_{14N(n,disap)}$-macro cross section is shown as dark blue circles ● at $E_n \lesssim 0.01$ MeV. (d) Dependence of the relation $\sigma^{macro}_{14N(n,p)14C}$ to the $\sigma^{macro}_{disap}(\mathrm{Air})$ from the energy. The all macro cross sections (in a–d-figures) are given for the altitude $H = 0$ at the sea level. In the figures for better visualization, the dependencies are given in two energy scales.

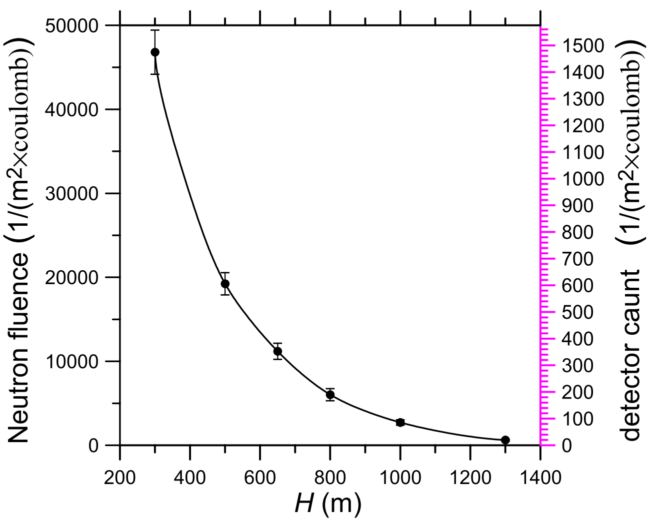

Figure 5. Dependence of neutron fluences on the ground (10 m above the sea level) from the altitude H of the lightning discharge (see the left vertical axis). Simulation is realized for the ground position for polar angle of registration $\pi/2$ (at the nadir point in the strict sense). The fluences correspond to one coulomb discharge. The number of expected counts per one square meter in the detector (with efficiency 0.0315) is given on the right axis.

of thunderclouds $H \simeq 7$ km (Rakov & Uman, 2005). Then, Y^{R1}_{C-14} (g-mole/year) $\simeq 1.7 \times 10^{-14} \times 20 \times 1.4 \times 10^{9} \simeq 5 \times 10^{-4}$ for the relation *R1*.

Similarly, it was simulated the yield of radioactive ^{41}Ar produced in air (simultaneously with ^{14}C) at neutron activation of the argon ^{40}Ar(n,γ)^{41}Ar. Its creation per mean flash (20 coulomb) is Y^{R1}_{Ar-41}(g-mole) $\simeq 2.9 \times 10^{-17} \times 20 \simeq 5.8 \times 10^{-16}$ for *R1* value. Owing to relevant ^{41}Ar decay parameters [$T_{1/2} = 109.34$ m, β^- (100%)], it will be attractive to consider this isotope as an appropriate tracer of the radiocarbon ^{14}C generation. In spite of the debugged technique of ^{41}Ar monitoring (for example for accelerators and reactors (Cicoria et al., 2017; Oyama et al., 2021), the detection of such low and changing ^{41}Ar concentration is a very complicated task. But it is possible that the detection will be more realistic in the case of gigantic terrestrial gamma flashes—the large-scale atmospheric phenomena in which population of neutrons exceeds the $\sim 10^{15}$ level (Babich, 2006).

4. Discussion

4.1. Could the Storm Radiocarbon Yield Be Strongly Larger?

The obtained yields of ^{14}C are evaluated based on the relation value *R1* $\simeq 1.3 \times 10^4$ (Dwyer & Babich, 2011). Today, there are two principal scenarios of electron avalanche (Dwyer & Babich, 2011; Gurevich et al., 2006). According to the alternative scenario of the electron avalanche (Gurevich et al., 2006), the relation value is *R2* $\simeq 3 \times 10^6$, which is more than that reported in the study by Dwyer & Babich, 2011 by a factor of two orders $k = 3 \times 10^6/1.3 \times 10^{4}$ (see also comments in Dwyer & Babich, 2012; Gurevich et al., 2012); this indicates the decrease of the obtained ^{14}C production in k times: Y^{R2}_{C-14} is equal to Y^{R1}_{C-14} / k and can be considered as the lower limit of ^{14}C yields. In contrast, the Y^{R1}_{C-14} value corresponds to the upper limits of radiocarbon creation.

Compared with the cosmogenic radiocarbon creation, the obtained ^{14}C yield under thunderstorm conditions is small: its part is equal to $(5 \times 10^{-4})/472 \simeq 1 \times 10^{-6}$ for 20-coulomb-charge of flashes. An unimportance of thunderstorm ^{14}C yield is also agreed with the increase of radiocarbon in tree rings in the time distance 774–775 CE at intensive Sun activity (Miyake et al., 2012). Indeed in the case of large ^{14}C yield under conditions of thunderstorms, the events with increased tree-ring-radiocarbon will be smeared, and yields from thunderstorms and Sun will be competed. But the solar particles ensure only about 0.25% from the global radiocarbon creation (Kovaltsov et al., 2012) that confirms an insignificance of ^{14}C yield at thunderstorms.

4.2. Comparison With the Experiment

With the purpose to test the neutron creation and neutron transport (as the key mechanisms of ^{14}C generation), it is important to compare the radiation transport results with events of correlated excess for neutron fluxes at thunderstorms. During thunder activity at the Ohi Power Station (near Japan sea), the detector PANDA36 had registered three strong radiation events and one of them (burst-20120105) correlated with excess of neutron counts (Kuroda et al., 2016). To reproduce the burst sources, the authors simulated the events at the combination of height H: 100, 500, 900, and 1,300 m (Kuroda et al., 2016). For evaluation of the possible altitudes of the event similar to neutron burst 20120105 (i.e., with the same neutron excess during the time duration 16 s, Kuroda et al., 2016), neutron fluences were calculated at the ground level (with polar angle of registration $\pi/2$) from the sources at $H = 300$, 500, 650, 800, 1000, and 1300 m above the sea level. The obtained fluences are normalized on the coulomb of the discharge (see the left vertical axis of Figure 5). The right vertical axis of Figure 5 shows the expected total counts when the detector efficiency is 3.15%. The results are in general agreement (or at least in rough agreement) with the experimental results.

So, for example, the neutron excess of ~260 events (as in burst-20120105) can be registered from ~1.5 coulomb discharge at altitude $H = 800$ m or at $H = 1$ km in the case of 3 coulomb discharge. Note that in the report (Kato, 2015), the authors indicated the probable height 400 m for the burst 20120105.

5. Conclusions

The gross model for evaluation of the radiocarbon ^{14}C yield under conditions of thunderstorm is proposed and its generation is simulated depending on the altitude up to 15 km above the sea level. The obtained results allow us to conclude that in the case of the relation $R1 \simeq 10^4$ of low energy electrons N_{le} to the relativistic ones N_{re} in the discharge avalanche (according to the avalanche scenario of Dwyer & Babich, 2011), the yield of ^{14}C isotope under thunderstorms adds up to $1 \times 10^{-4}\%$ to the radiocarbon creation from the cosmogenic irradiation that can be considered as the upper limit of radiocarbon production from thunderstorm flashes. In the alternative scenario of the relation $R2 = N_{le}/N_{re} \simeq 3 \times 10^6$ (of the work (Gurevich et al., 2006), the yield of ^{14}C isotope will be two orders less. The considered scenarios of ^{14}C production indicate the negligible contribution of the thunderstorm radiocarbon to the total creation in the Earth's atmosphere that allows us to eliminate the problematic issue on the dating correction caused by the thunderstorm mechanism.

Data Availability Statement

The nuclear data (see Figure 2, Table S1) are accessible in https://www.oecd-nea.org/janisweb/search/endf, https://www.nndc.bnl.gov/sigma/ and in repositorium https://data.mendeley.com/datasets/dktf9fkwdb/1, https://doi.org/10.17632/dktf9fkwdb.1.

Acknowledgments
The author thanks I. N. Borzov for helpful and useful discussion.

References

Babich, L. P. (2006). Generation of neutrons in giant upward atmospheric discharges. *JETP Letters*, *84*, 285–288. https://doi.org/10.1134/S0021364006180020

Babich, L. P. (2017a). Radiocarbon Production by Thunderstorms. *Geophysical Research Letters*, *44*(11), 11191–11200. https://doi.org/10.1002/2017GL075131

Babich, L. P. (2017b). Thunderous nuclear reactions. *Nature*, *551*, 443–444. https://doi.org/10.1038/d41586-017-07266-w

Babich, L. P., & Roussel-Duprè, R. A. (2007). Origin of neutron flux increases observed in correlation with lightning. *Journal of Geophysical Research*, *112*, D13303. https://doi.org/10.1029/2006JD008340

Chilingarian, A., Hovsepyan, G., & Vanyan, L. (2014). On the origin of the particle fluxes from the thunderclouds: Energy spectra analysis. *Europhysics Letters*, *106*(5), 59001. https://doi.org/10.1209/0295-5075/106/59001

Chilingarian, A., Daryan, A., Arakelyan, K., Hovhannisyan, A., Mailyan, B., Melkumyan, L., et al. (2010). Ground-based observations of thunderstorm-correlated fluxes of high-energy electrons, gamma rays, and neutrons. *Physical Review D*, *82*, 043009. https://doi.org/10.1103/PhysRevD.82.043009

Christian, H. J., Blakeslee, R. J., Boccippio, D. J., Boeck, W. L., Buechler, D. E., Driscoll, K. T., et al. (2003). Global frequency and distribution of lightning as observed from space by the Optical Transient Detector. ACL 4-1-ACL 4-15. *Journal of Geophysical Research*, *108*. https://doi.org/10.1029/2002JD002347

Cicoria, G., Cesarini, F., Infantino, A., Vichi, S., Zagni, F., & Marengo, M. (2017). Characterization of 41Ar production in air at a PET cyclotron facility. *Modern Physics Letters A*, *32* (17), 1740014-1–1740014-14. https://doi.org/10.1142/S0217732317400144

COESA Working Group. (1976). *U.S. Standard atmosphere*, (National Aeronatic and Space Administration). NASA-TM-X-74335. Retrieved from https://www.ngdc.noaa.gov/stp/space-weather/online-publications/miscellaneous/us-standard-atmosphere-1976/us-standard-atmosphere_st76-1562_noaa.pdf

Dwyer, J. R., & Babich, L. P. (2011). Low-energy electron production by relativistic runaway electron avalanches in air. *Journal of Geophysical Research*, *116*, A09301. https://doi.org/10.1029/2011JA016494

Dwyer, J. R., & Babich, L. P. (2012). Reply to comment by A. V. Gurevich et al. on "Low-energy electron production by relativistic runaway electron avalanches in air". *Journal of Geophysical Research*, *117*, A04303. https://doi.org/10.1029/2011JA017487

ENDF-7u. (2008). *ENDF7u photonuclear library of RSICC CODE PACKAGE CCC-740*. Retrieved from https://www-rsicc.ornl.gov/codes/ccc/ccc7/ccc-740.html

Enoto, T., Wada, Y., Furuta, Y., Nakazawa, K., Yuasa, T., Okuda, K., et al. (2017). Photonuclear reactions triggered by lightning discharge. *Nature*, *551*, 481–484. https://doi.org/10.1038/nature24630

Gerst, S. S., & Quay, P. (2000). The deuterium content of atmospheric molecular hydrogen: Method and initial measurements. *Journal of Geophysical Research*, *105*(D21), 26433–26445. https://doi.org/10.1029/2000JD900387

Gunn, R. (1948). Electric field intensity inside of natural clouds. *Journal of Applied Physics*, *19*, 481–484. https://doi.org/10.1063/1.1698159

Gurevich, A. V., Milikh, G. M., & Roussel-Dupre, R. (1992). Runaway electron mechanism of air breakdown and preconditioning during a thunder storm. *Physics Letters A*, *165*, 463–468. https://doi.org/10.1016/0375-9601(92)90348-P

Gurevich, A. V., Roussel-Dupre, R., Zybin, K. P., & Milikh, G. M. (2012). Comment on "Low-energy electron production by relativistic runaway electron avalanches in air" by J. R. Dwyer and L. P. Babich. *Journal of Geophysical Research*, *117*, A04302. https://doi.org/10.1029/2011JA017431

Gurevich, A. V., Zybin, K. P., Medvedev, Y. V., & Yu, V. (2006). Amplification and nonlinear modification of runaway breakdown. *Physics Letters A*, *349*, 331–339. https://doi.org/10.1016/j.physleta.2005.09.074

Ishtiaq, P. M., Mufti, S., Darzi, M. A., Mir, T. A., & Shah, G. N. (2016). Observation of 2.45 MeV neutrons correlated with natural atmospheric lightning discharges by Lead-Free Gulmarg Neutron Monitor. *Journal of Geophysical Research: Atmospheres*, *121*, 692–703. https://doi.org/10.1002/2015JD023343

Iwamoto, N., Kosako, N., & Murata, T. (2016). Photonuclear data file. In: *Proceedings of the 2015 Symposium on Nuclear Data. November 19-20, 2015, Ibaraki Quantum Beam Research Center, Tokai-mura*, JAEA-Conf 2016-004. INDC(JPN)-202, (pp. 53–58). https://doi.org/10.11484/jaea-conf-2016-004. Retrieved from https://jopss.jaea.go.jp/pdfdata/JAEA-Conf-2016-004.pdf

Kato, Y. (2015). Thundercloud-related radiation bursts observed at a coastal area and a mountaintop using a segmented organic scintillators. *Paper Presented at International Symposium at the Yerevan Physics Institute*, October 5-9, 2015, TEPA-2015, Byurakan, Aragatsotn District, Armenia. Retrieved from http://crd.yerphi.am/Conferences/tepa2015/files/presentations/Oct7/20151007_TEPA2015_ykato.pdf

Kovaltsov, G. A., Mishev, A., & Usoskin, I. G. (2012). A new model of cosmogenic production of radiocarbon ^{14}C in the atmosphere. *Earth and Planetary Science Letters*, *337–338*, 114–120. https://doi.org/10.1016/j.epsl.2012.05.036

Kuroda, Y., Oguri, S., Kato, Y., Nakata, R., Inoue, Y., Ito, C., & Minowa, M. (2016). Observation of gamma ray bursts at ground level under the thunderclouds. *Physics Letters B*, *758*, 286–291. https://doi.org/10.1016/j.physletb.2016.05.029

Kuzhevskii, B. M. (2004). Neutron production in lightnings. *Vestnik Moskovskogo Universiteta, Seriya 3: Fiz. Astron*, *5*, 17.

Libby, L. M., & Lukens, H. R. (1973). Production of radiocarbon in tree rings by lightning bolts. *Journal of Geophysical Research*, *78*(26), 5902–5903. https://doi.org/10.1029/JB078i026p05902

Miyake, F., Nagaya, K., Masuda, K., & Nakamura, T. (2012). A signature of cosmic-ray increase in ad 774–775 from tree rings in Japan. *Nature*, *486*, 240–242. https://doi.org/10.1038/nature11123

Oyama, T., Nagaguro, S., Hagiwara, M., Nakamura, H., Shirakata, M., Saito, K. & Yamazaki, H. (2021). Measurements and characterization of air activation in J-PARC main ring. In: JPS Conference Proceedings, (pp. 011147-1–011147-6). https://doi.org/10.7566/JPSCP.33.011147

Rakov, V. A., & Uman, M. A. (2005). *Lightning: Physics and effects*. Cambridge University Press (ISBN: 9780521035415).

Roth, R., & Joos, F. (2013). A reconstruction of radiocarbon production and total solar irradiance from the Holocene 14C and CO_2 records: Implications of data and model uncertainties. *Climate of the Past*, *9*, 1879–1909. https://doi.org/10.5194/cp-9-1879-2013

Rozansky, K., & Sonntag, C. (1982). Vertical distribution of deuterium in atmospheric water vapour. *Tellus*, *34*, 135–141. https://doi.org/10.3402/tellusa.v34i2.10795

Shah, G. N., Razdan, H., Bhat, C. L., & Ali, Q. M. (1985). Neutron generation in lightning bolts. *Nature*, *313*, 773–775. https://doi.org/10.1038/313773a0

Shibata, K., Kawano, T., Nakagawa, T., Iwamoto, O., Katakura, J., Fukahori, T., et al. (2002). Japanese Evaluated nuclear data library Version 3 Revision-3: JENDL-3.3. *Journal of Nuclear Science and Technology*, *39*, 1125–1136. https://doi.org/10.1080/18811248.2002.9715303

Shyam, A., & Kaushik, T. C. (1999). Observation of neutron bursts associated with atmospheric lightning discharge. *Journal of Geophysical Research*, *104*, 6867–6869. https://doi.org/10.1029/98JA02683

Starodubtsev, S. A., Kozlov, V. I., Toropov, A. A., Mullayarov, V. A., Grigor'ev, V. G., & Moiseev, A. V. (2012). First experimental observations of neutron bursts under thunderstorm clouds near sea level. *JETP Letters*, *96*, 188–191. https://doi.org/10.1134/S0021364012150106

Suess, H. E. (1965). Secular variations of the cosmic-ray-produced carbon 14 in the atmosphere and their interpretations. *Journal of Geophysical Research*, *70*, 5937–5952. https://doi.org/10.1029/JZ070i023p05937

Wilson, C. T. R. (1925). The acceleration of β-particles in strong electric fields such as those of thunderclouds. *Mathematical Proceedings of the Cambridge Philosophical Society*, *22*, 534–538. https://doi.org/10.1017/S0305004100003236

Winn, W. P., Schwede, G. W., & Moore, C. B. (1974). Measurements of electric fields in thunderclouds. *Journal of Geophysical Reseach*, *79*, 1761–1767. https://doi.org/10.1029/JC079i012p01761

References From the Supporting Information

Brown, D. A., Chadwick, M. B., Capote, R., Kahler, A. C., Trkov, A., Herman, M. W., et al. (2018). ENDF/B-VIII.0: The 8th major release of the nuclear reaction data library with CIELO-project cross sections, new standards and thermal scattering data. *Nuclear Data Sheets*, *148*, 1–142. https://doi.org/10.1016/j.nds.2018.02.001

ENDF-6 Formats Manual. (2009). Data formats and procedures for the evaluated nuclear data files ENDF/B-VI and ENDF/B-VII. CSEWG Document ENDF-102. *Written by the Members of the Cross Sections Evaluation Working Group*, Edited by In M. Herman and A. Trkov. National Nuclear Data Center Brookhaven National Laboratory. Retrieved from https://www.oecd-nea.org/dbdata/data/manual-endf/endf102.pdf

Koning, A. J., Rochman, D., Sublet, J., Dzysiuk, N., Fleming, M., & van der Marck, S. (2019). TENDL: Complete nuclear data library for innovative nuclear science and technology. *Nuclear Data Sheets*, *155*, 1–55. https://doi.org/10.1016/j.nds.2019.01.002

OECD/NEA Data Bank. (2005). *The JEFF-3.0 nuclear data library*. JEFF Report 19. OECD/NEA Data Bank. Retrieved from https://www.oecd-nea.org/jcms/pl_14080

Sublet, J.-C., Packer, L. W., Kopecky, J., Forrest, R. A., Koning, A. J., & Rochman, D. A. (2010). The European Activation File: EAF-2010 neutron-induced cross section library. In: *EASY Documentation Series, CCFE-R* (10) 05. Retrieved from https://t2.lanl.gov/nis/data/jeff/EAF2010.pdf